# INNOVATIVE ALGINATE-BASED HYBRID COMPOSITE BEADS FOR HEAVY METALS REMOVAL

Andreea MIRON[1,2], Andrei SARBU[3], Teodor SANDU[4], Ana-Mihaela Gavrila[5], Anda Maria BAROI[6], Anita-Laura CHIRIAC[7*], Tanta-Verona IORDACHE[8], Horia IOVU[9*]

*Nowadays, heavy metal pollution is considered one of the most important environmental issues. Thereby, this paper proposes a novel approach towards obtaining biofriendly hybrid composite beads based on sodium alginate-type biopolymer incorporating inorganic-organic composite synthetized through host-guest polymerization of polyacrylonitrile within a porous titania structure. Firstly, optimal synthesis procedure for developing composites with improved characteristics was established. The new systems were characterized by FTIR, XRD, TGA and SEM. The performed heavy metal adsorption tests indicated that the alginate matrix presents a higher affinity for Cu ions, relative to Zn and Ni ions and a higher efficiency relative to the reference $TiO_2$ beads.*

**Keywords**: titania, host-guest polymerization, sodium alginate, hybrid composite beads, heavy metals

## 1. Introduction

We are currently dealing with a global environmental issue, related to the contamination of water. This pollution effect is mainly caused by heavy metals, as they are bio cumulative and pose deleterious effects on humans [1-2]. In this context, innovative means of water treatment must be developed. Adsorption processes have recently gained the interest of researchers due to their advantages over conventional treatment methods [1-3].

[1] Scientific Researcher, PhD Student., National Institute for Research & Development in Chemistry and Petrochemistry ICECHIM, Bucharest, Romania, e-mail: andreea.miron@icechim.ro
[2] Scientific Researcher, PhD Student., Dept. of Polymer Science, The National University of Science and Technology POLITEHNICA Bucharest, Romania, e-mail: andreea.miron@icechim.ro
[3] National Institute for Research & Development in Chemistry and Petrochemistry ICECHIM, Romania
[4] National Institute for Research & Development in Chemistry and Petrochemistry ICECHIM
[5] National Institute for Research & Development in Chemistry and Petrochemistry ICECHIM
[6] National Institute for Research & Development in Chemistry and Petrochemistry ICECHIM
[7] National Institute for Research & Development in Chemistry and Petrochemistry ICECHIM *corresponding author e-mail: anita-laura.radu@icechim.ro
[8] National Institute for Research & Development in Chemistry and Petrochemistry ICECHIM
[9] Dept. of Polymer Science, The National University of Science and Technology POLITEHNICA Bucharest, Romania, *corresponding author's e-mail: horia.iovu@upb.ro

Inorganic-organic composites have been extensively studied for a long time because of their remarkable properties [4]. Recent technological advances, together with the search for materials with new characteristics, have led to significant advances developing new materials with improved properties. The ability to take benefit of the characteristics of both inorganic and organic components to generate new material with superior attributes is the main advantage of inorganic-organic hybrids [5]. Due to the remarkable improvements in the mechanical, thermal, electrical, and magnetic features versus the pure organic polymers, inorganic-organic composites have received tremendous attention [5-9]. The synthesis, as well as the use of inorganic-organic composites has experienced an accelerated development in the last decade. Porous materials, including zeolites (pore diameter < 2 nm) and mesoporous materials (pore diameter 2 - 50 nm), are used as inorganic hosts, as their composition and structure are versatile and multiple guest species, such as synthetic polymers can be encapsulated; thus, complex materials with improved properties being formed [9-10]. The sol-gel process is among the most widely used processes for the synthesis of this kind of materials, as it allows for the inorganic network formation, the incorporation of dense inorganic structures already obtained, but also the formation of hybrids using layered or porous inorganic materials, either by the interpenetration of organic polymers in voids, or by exfoliation of the inorganic material [11]. Synthesis of polymer hybrids is straightforward and low-cost, and the precursors are also affordable, while the production process can be easily implemented industrially [12]. Therefore, it can also be assumed that the final materials are cost-effective.

Hybrid composite beads have also attracted the attention of recent researchers due to the ability to combine the individual benefits of several materials into single, a innovative material, without involving high costs and complex technologies [13]. In general, the matrix of polymeric beads consists of an inorganic compound or an inorganic-organic composite in both cases having the role of enhancing the adsorption capacity of the beads. In order to be more environmentally friendly, polymeric beads are generally made from biopolymers, such as alginate or chitosan, which are extracted from renewable and environmentally friendly sources and are well-known for their ability to retain various pollutants. The adsorption capacity towards heavy metals may increase significantly when adding certain inorganic fillers such as zeolites, titanium dioxide, carbon nanotubes, and magnetic powders [13-15].

Composite materials based on an organic alginate matrix have been intensively studied in several fields (water treatment, pharmaceutical and cosmetic industry, agriculture, etc.) because they have significantly improved characteristics compared to synthetic polymers, such as abundance in nature, biocompatibility, and biodegradability. Researchers have brought to attention polymer composite beads because their manufacturing technology is simple and does not involve high costs.

At the same time, using hybrid polymer beads on an industrial scale is much more advantageous and straightforward than using powders [16-17].

In this context, this work aimed at developing new composite materials with advanced capacity to retain heavy metals from water. Therefore, we report a novel approach for obtaining simple and inexpensive hybrid beads based on sodium alginate-type biopolymer containing inorganic-organic composite synthesized through host-guest polymerization of polyacrylonitrile within a porous titanium oxide structure. To the best of our knowledge, such innovative systems incorporating host-guest composite fillers have not been reported before. Therefore, this study comprises two parts, the first part is dedicated to optimizing the synthesis process of inorganic-organic composites by the host-guest method, whereas the second part deals with the preparation and characterization of the new alginate-based hybrid composite beads.

## 2. Experimental section

### *2.1. Materials*

In this study, inorganic-organic composites were prepared using titanium oxide-titania ($TiO_2$, type $MZ_{48}$) as raw material. Mesoporous titania (fine powder; particle size of -150 + 75 μm) was kindly provided by National Institute for Research and Development in Electrochemistry and Condensed Matter, Timisoara; the inorganic matrix was obtained by a microwave hydrothermal method and hexadecylamine as a surfactant. The vinyl monomer, Acrylonitrile (AN, 99%, Fluka) was distilled in order to remove the polymerization inhibitor and stored in the refrigerator (at temperatures not exceeding 5 °C). The radical polymerization initiator, azo-bis-isobutyronitrile (AIBN, 99%, Fluka) was used as received. The biopolymer, sodium alginate (SA), and the coagulation agent, calcium chloride ($CaCl_2$, 0.25M), both from Sigma-Aldrich, were used as received for the preparation of hybrid beads. Copper/ nickel/ zinc sulphate for analysis (>99% purity) were purchased from Merck.

### *2.2. Methods*

#### *2.2.1. Synthesis of inorganic-organic composites*

The inorganic-organic composites were prepared similarly to a previously published work [18]. The synthesis process of host-guest hybrids involves two steps: (i) impregnation/adsorption of AN in the pores of mesoporous titania, and (ii) AN polymerization, thus obtaining polyacrylonitrile (PAN) in the pores of the inorganic host, both assisted by ultrasound. In order to optimize the synthesis process, four different composite samples were synthesized varying the impregnation/adsorption time (at room temperature) and the polymerization time (at 65 °C). The ratio between inorganic and organic phases was 30-70 (wt.%). The

prepared composites with the compositions given in Table 1 were noted as $30MZ_{48}$-xhUS, where x represents the impregnation time (h). Additionally, radical polymerization of acrylonitrile in the absence of inorganic host was also performed. The reference PAN was obtained by introducing the acrylonitrile into a glass ampoule together with AIBN initiator (1%) at a temperature of 65 °C for 24 h, in ultrasonic field.

*Table 1*

**Composition of inorganic-organic composites particles**

| Sample | Organic (wt.%) | Inorganic (wt.%) | Impregnation time (h) | Polymerization time (h) |
|---|---|---|---|---|
| **$30MZ_{48}$-6hUS** | 70 | 30 | 6 | 12 |
| **$30MZ_{48}$-8hUS** | 70 | 30 | 8 | 8 |
| **$30MZ_{48}$-12hUS** | 70 | 30 | 12 | 12 |
| **$30MZ_{48}$-24hUS** | 70 | 30 | 24 | 24 |

### *2.2.2. Synthesis of hybrid composite beads*

Reference sodium alginate beads (SA), sodium alginate-based titania (SA-Ti) beads and sodium alginate-based hybrid composite (SA-Ti_PAN) beads were prepared as described in the next few lines. Sodium alginate was dissolved in distilled water (3% w/v). To obtain the hybrid materials, as depict in Fig. 1, a specific amount of 0.1 mg of mesoporous titania/composite powder was introduced in the sodium alginate solution. The mixture was stirred at 40 °C (4 h; 200 rpm) and left until the solution became homogeneous, without bubbles. Reference alginate or titania/composite beads were obtained by dropping this solution through a syringe needle into a 0.25M $CaCl_2$ solution under gentle magnetic stirring (50 rpm). The formed spherical beads were kept in $CaCl_2$ solution for 12 h, then were filtered and washed with distilled water for 3 times. The samples were dried by lyophilization at a temperature of -70 °C.

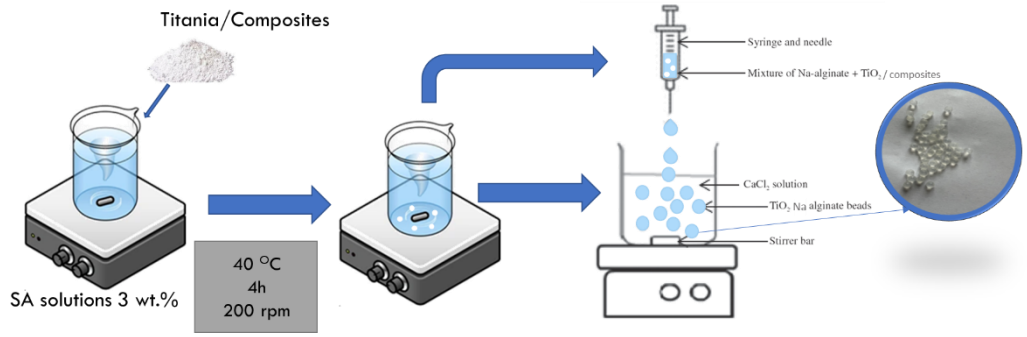


Fig 1. Schematic representation of hybrid composite beads preparation

### *2.2.3. Adsorption tests*

In order to determine the adsorption capacity of the alginate-based hybrid composite materials, tests were carried out by immersing 20 mg of hybrid beads in

20 mL of heavy metal solution (copper/ nickel/ zinc sulphate) with a concentration of 300 mg/L. The tubes were placed in a shaker (MultiTherm Shaker BENCHMARK SCIENTIFIC) at a speed of 200 rpm for a period of 24 hours. After this step, the samples were milled and submitted to X-ray fluorescence (XRF) analysis to evaluate the adsorbed content of heavy metals.

### *2.3. Characterization techniques*

The prepared host-guest composite particles and hybrid composite beads were structurally, morphologically, and thermally characterized using various tools and methods. *Fourier Transform Infrared (FTIR)* spectra of the samples were recorded on a Nicolet ™ Summit PRO FTIR Spectrometer- ThermoFisher Scientific, using 16 scans in the 4000-600 $cm^{-1}$ range with a resolution of 4 $cm^{-1}$. *Brunauer–Emmett–Teller (BET)* and *Barrett–Joyner–Halanda (BJH) methods* were used to measure the specific surface areas and pore size distributions of raw titania and host-guest composites at 77.4 K (-196 °C) using a Quantachrome Nova2200e Analyzer. Prior to measurements, samples were degassed at 373.15 K for 3h under vacuum (p <102 Pa). *Thermal Gravimetric Analysis/Differential Thermal Gravimetry (TGA/DTG)* curves were recorded using a TG 209 F1 Libra, Netzsch instrument by heating 5-10 mg samples from 20 °C to 700 °C at a heating rate of 10 °C/min, under a nitrogen flow, using a Platinum/Rhodium crucible. *Dynamic Mechanical Analysis (DMA)* of the polymer and prepared composites was undertaken using a TRITEC 2000 B analyzer. The samples were analyzed on a powder clamp and the damping factor (tan δ) was recorded as a function of temperature from 25 to 200 °C at a heating rate of 5 °C/min. *X-ray diffraction (XRD)* patterns of hybrid beads were collected with a Rigaku SmartLab equipment, operated at 45 kV and 200 mA, with Cu Kα radiation (wavelength λ = 0.1541 nm) in parallel beam configuration (2θ/θ scan mode). The scanned range was 2 h = 2–60°, with a scan rate of 1°/min. *Scanning Electron Microscope (SEM)* images of analyzed samples were pointed out using the Hitachi TM4000plus II tabletop, with one cooling step. *X-ray fluorescence (XRF)* spectra were recorded using a Vanta C Series Handheld device. Analyzer includes rhodium (Rh) anode 40 kV X-ray tube, SDD (Silicon Drift Detector), in-line camera for aiming, 3mm X-ray spot collimation and 5-megapixel sample camera for documenting tests.

## 3. Results and discussions

### *3.1. Optimization of inorganic-organic composites synthesis by the host-guest method*

The innovative host-guest polymerization technique for obtaining inorganic-organic composites involving ultrasonication in both stages of adsorption/impregnation of acrylonitrile in the titania mesopores and the

subsequent polymerization of the vinyl monomer can result in substantial improvements of mechanical and thermal properties of the final materials. Therefore, different parameters as impregnation or polymerization time were varied to obtain homogenous structures incorporating PAN chains able to fit very well in the $TiO_2$ pores. For this reason, the first stage of this research aimed to optimize the composite synthesis process by establishing the optimal synthesis procedure for developing composites with improved characteristics.

### *3.1.1. FTIR structural analysis of composite materials*

FTIR spectroscopy was used to investigate the chemical structure of inorganic-organic composites developed from mesoporous titania and PAN. Fig. 2 illustrates the spectra of $MZ_{48}$ titania-based composites with an inorganic phase content of 30% ratio and different impregnation/polymerization times. According to Fig. 2, all samples showed similarities in terms of main characteristic bands.

The characteristic spectrum of the reference PAN shows bands at 1246, 1353, 1452 $cm^{-1}$ regions, which are representative of C-H vibrations. The band at 1455 $cm^{-1}$ is associated with the deformation vibration of $CH_2$ [19]. The presence of residual monomer is confirmed by the existence of bands at 1621 $cm^{-1}$, 1071 $cm^{-1}$, and 1353 $cm^{-1}$, which are attributed to the stretching vibrations of C=C, C-C, and C-H in alkenes structure. The characteristic bands of the C≡N group and C-H group can be detected at 2245 $cm^{-1}$ and 2945 $cm^{-1}$, respectively.

Compared to the spectrum of pure PAN, the spectra of all nanocomposites exhibit bands corresponding to the stretching vibrations of methylene groups. Stretching vibrations at 2860 and 2934 $cm^{-1}$ can be attributed to C-H bond vibrations of the organic polymer developed inside the titania. Moreover, the FTIR spectra of host-guest composites show bands at 2243 $cm^{-1}$ corresponding to the CN group of PAN.

When comparing the composites prepared using shorter impregnation/ultrasonication times to the reference polymer, higher intensities of bands can be observed. Additionally, in the case of these systems, the monomer seems well incorporated, with specific polymer bands (2934, 2860 and 2245 $cm^{-1}$) of higher intensity than the other systems analysed. This validates the full monomer conversion, eliminating any uncertainty about the presence of the unreacted monomer, beneficial for the homogeneity of the final composites.

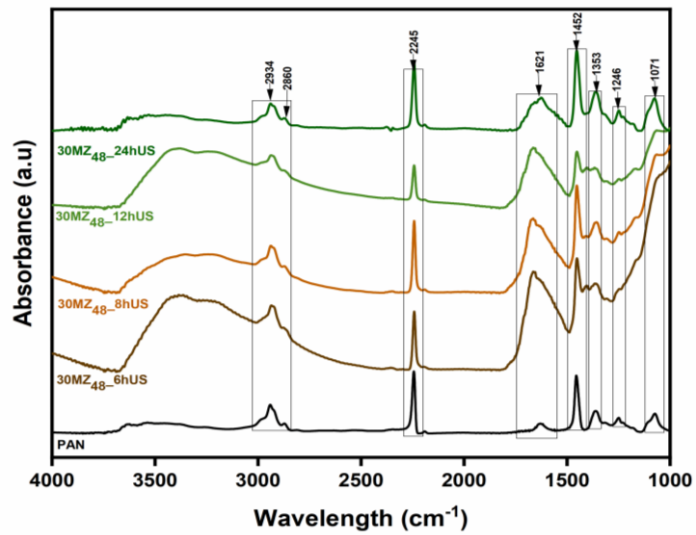


Fig 2. FTIR spectra for the reference polymer and composites

### *3.1.2. Porosimetry Measurements*

Particle size and surface porosity are important parameters for adsorbent systems, since small sorbent sizes increase the specific surface area ($m^2/g$), while high porosity increases the external surface area. The combination of both parameters simultaneously improves the actual surface area [20]. As indicated in Table 2, the specific titania and synthesized composite surface area, pore volume, and pore size were calculated using the adsorption isothermal data. For $MZ_{48}$ type titania, the BET surface area is 128.3 $m^2g^{-1}$, while the synthesized composites attained values between 52.99 and 1.7 $m^2g^{-1}$. In the case of synthesized titania-acrylonitrile composites, the polymer formation is observed in the pores of the host titania in which the pore diameter was around 7 nm, with exception for $30MZ_{48}$-6hUS composite, which registered a pore diameter of 4.7 nm. Average pore diameters fall within the domain of mesoporous materials. It can also be noted that the increase of the ultrasonication time leads to higher surface areas and pore surface area of composites. As a concluding remark, the results confirm the presence of the polymer in the guest pores of titania, which indicate that the polymerization process was successful.

*Table 2*

**Textural characteristics of composites materials**

| Sample | Surface area (BJH) ($m^2$ $g^{-1}$) | Pore surface area (BJH) ($m^2$ $g^{-1}$) | Pore diameter in desorption (BJH) (nm) | Pore volume (BJH) (measured at P/P0 = 0.99) ($cm^3$ $g^{-1}$) |
|---|---|---|---|---|
| **$MZ_{48}$** | 128.3 | 140.9 | 7.7 | 0.2864 |
| **$30MZ_{48}$-24hUS** | 52.9 | 72.6 | 7.1 | 0.1272 |

| | | | | |
|---|---|---|---|---|
| **30MZ$_{48}$-12hUS** | 22.3 | 31.4 | 7.1 | 0.0565 |
| **30MZ$_{48}$-8hUS** | 24.9 | 33.7 | 7.1 | 0.0059 |
| **30MZ$_{48}$-6hUS** | 1.7 | 1.8 | 4.7 | 0.0033 |

### *3.1.3. Thermal and mechanical properties of the ~~for~~ composite materials*

The influence of impregnation /polymerization time on the thermostability of synthesized systems was investigated using thermogravimetric analysis (TGA) and differential thermogravimetric analysis (DTG). In order to gain a better insight into composite systems, the results were compared with those of the reference polymer (PAN). Figs. 3(a) and Fig. 3(b) show the TGA the DTG curves, respectively, of the reference titania, polymer and the $MZ_{48}$ titania-based composite materials. Table 3 summarizes the values of the glass transition and the cyclization temperature, decomposition temperatures ($T_d$) and mass losses for each degradation stage.

*Table 3*

**Thermal and mechanical properties of the samples**

| **Sample** | ***TGA*** | | | | ***DMA*** | **DSC** |
|---|---|---|---|---|---|---|
| | **$T_{d1}$, °C** | **$T_{d2}$, °C** | **$T_{d3}$, °C** | **Weight loss, %** | ***Tg, °C*** | ***$T_{cyclization}$, °C*** |
| **$MZ_{48}$** | - | - | - | 4.55 | - | - |
| **PAN** | 280.73 | 353.79 | 413.33 | 41.87 | 102.98 | 265.32 |
| **30MZ$_{48}$-24hUS** | 285.80 | – | 417.05 | 25.93 | 119.58 | 261.89 |
| **30MZ$_{48}$-12hUS** | 283.51 | - | 420.15 | 19.40 | 116.16 | 263.52 |
| **30MZ$_{48}$-8hUS** | 289.40 | - | 417.67 | 18.65 | 102.37 | 275.80 |
| **30MZ$_{48}$-6hUS** | 290.94 | - | 420.07 | 12.97 | 102.36 | 263.65 |

Polyacrylonitrile decomposition occurs in several stages. The increase in temperature leads to the decomposition of the polymeric structure. The first mass loss up to 280.73 °C, of 9.58%, is due to the cyclization reaction of the CN groups in a polyconjugate structure, followed by the aromatization process, at 353.79 °C, with the loss of hydrogen atoms and the formation of a conductive aromatic structure, with a mass loss of 6.68%. The last stage can be associated with aromatization, with a maximum temperature of 413.33 °C and a mass loss of 25.61%.

Compared to the PAN reference, for which the mass loss is 41.87%, the composites presented lower mass losses, which is partly attributed to the high thermal stability of mesoporous titania. The novel composite materials, with different impregnation/polymerization times, present two stages of degradation, as follows: the first one (150-300 °C), ascribed to the polyacrylonitrile cyclization reaction and the second one (300-440 °C), attributed to the aromatization processes of PAN [21].

It can be observed that the inorganic matrix shifts the cyclization maximum to higher temperatures, and the aromatization maximum decomposition

temperature is more flattened corresponding to two decomposition stages that were overlapping, corresponding to the two stages that overlapped and giving the aspect of a "hump". Hence, titania is a material that participates in the process, as evidenced by the rise in temperature and intensity of the cyclization peak.

The 6-hour interval is sufficient for monomer dispersion, and the heat degradation steps are well defined. Moreover, it seems that increasing the ultrasonication duration, leads to higher mass losses for the composite materials.

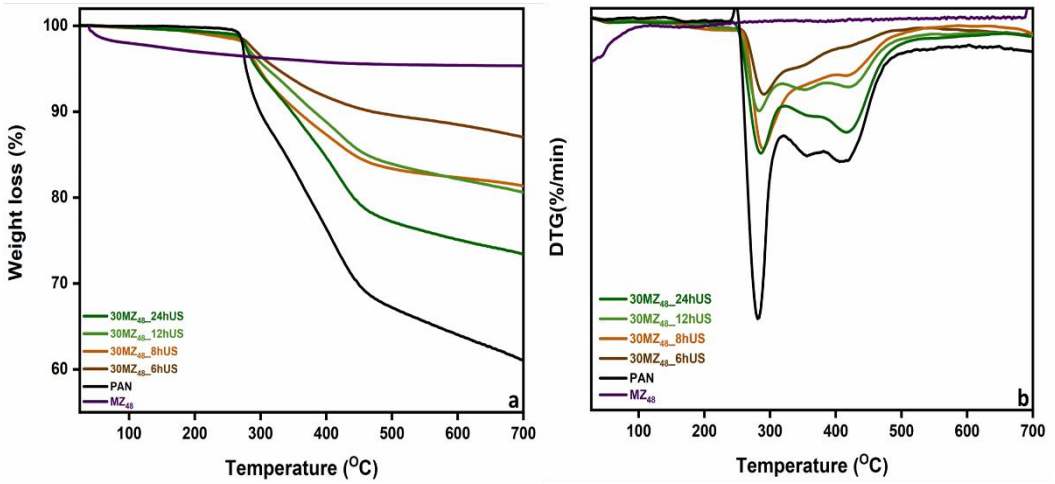


Fig 3. TGA(a) and DTG(b) curves of titania, reference polymer, and composites

The DMA showed one obvious glass transition temperature (around 100 °C for PAN and up to 119 °C for composites), regardless of the impregnation/polymerization time, demonstrating the formation of the polymer in titania mesopores, but also on its surface. It can be noted that the Tg increases with the increase of the ultrasonication time. The maximum value of tanδ for the composites was also found to be migrating to slightly higher temperatures than the reference polymer. Since decreasing the impregnation/polymerization time has no detrimental effect on the molecular dynamics of the polymer hybrids in the studied temperature range, we can conclude that the process can be improved by reducing the impregnation/polymerization time. According to the DSC analysis, ~~T~~the ~~second~~ exoterm registered at 265 °C for PAN and around 261-275 °C for the composites materials is attributed to the precursor reaction of thermal cyclization in PAN as described by [22].

Concludingly, incorporation of the polymer filler increases the dynamic properties of all the studied samples. According to the preliminary host-guest polymerization study, the optimal conditions to obtain cost-effective inorganic-organic composites with enhanced properties corresponded to the procedure consisting of only 6 hours for impregnation and 12 hours for polymerization, both

assisted by ultrasonication. In conclusion, the best composite obtained in this part of the study and further selected for the synthesis of composite beads (noted as SA-Ti_PAN) was 30MZ$_{48}$-6hUS.

### *3.2. Characterization of alginate-based hybrid composite beads*

#### *3.2.1. -Structure evaluation of composite beads*

Fig. 4a comparatively illustrates the FTIR spectra for alginate-based titania composite and hybrid composite beads. Both spectra show characteristic bands of sodium alginate. The stretching vibration of the O-H bond of sodium alginate can be observed around 3445 cm$^{-1}$. The aliphatic C-H group was recorded at a value of 2925 cm$^{-1}$, while the bands at 1612 cm$^{-1}$ and 1421 cm$^{-1}$ are attributed to the asymmetric and symmetric stretching vibrations of the carboxylate salt ion [23,24]. Compared to the composite with Ti alone (SA_Ti), the sample SA-Ti_PAN showed a band at 2243 cm$^{-1}$, characteristic of the cyano group (C≡N) in polyacrylonitrile (due to the presence of PAN in the filler, i.e., 30MZ$_{48}$-6hUS) [17].

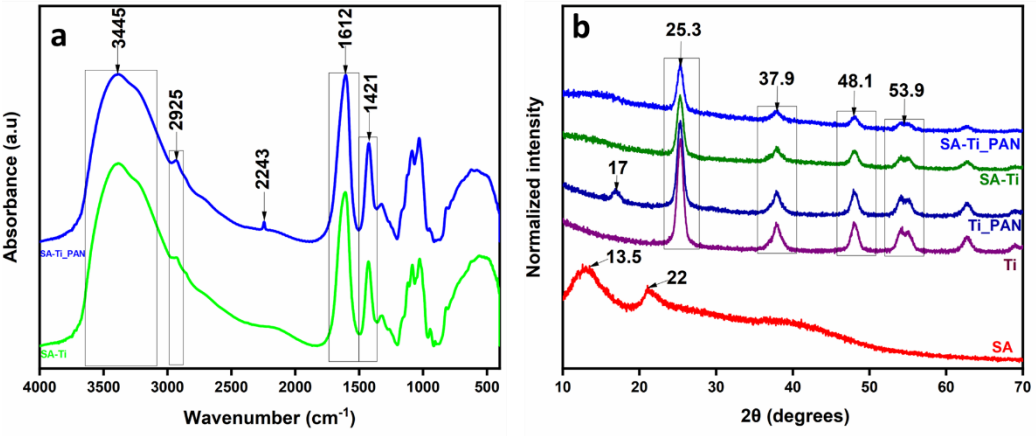


Fig 4. FTIR spectra of composite beads (a); XRD patterns of composite beads (b)

The XRD patterns (Fig. 4b) of the synthesized alginate and titania/composite beads show characteristic mesoporous bands for $TiO_2$. The sharp peaks at 2θ 25.3° correspond to the $TiO_2$ crystal with tetragonal structure, 37.9°, 48.1° 53.9°, being characteristic of the $TiO_2$ crystal planes of the anatase phase with good stability [25, 26]. The inorganic-organic composite (Ti_PAN) shows the characteristic peak of acrylonitrile around 17.0 and is attributed to the (100) plane of pure PAN polymer. Generally, sodium alginate has a semi-crystalline structure, due to hydrogen bonding interactions in the polymer chain. Two diffraction peaks can be observed at 2θ values of 13.5° and 22° due to the reflection from the (110) plane for polyguluronate units and the (200) plane for polymannuronate units [27].

### *3.2.2. Thermal stability of hybrid composite beads*

In order to determine the thermal stability of polymer composite bead samples, thermogravimetric analysis was carried out in the temperature range 30-700 ˚C and is presented in Fig. 5. TGA confirmed the presence of several degradation stages. The first mass loss in the 30-100 ˚C range is attributed to moisture evaporation, as reported in the literature [28], while the second stage of degradation recorded in the 200-270 ˚C region, is characteristic of sodium alginate. At this stage, a complex process of decomposition of the carboxylate group (COO-) into water takes place, releasing $CH_4$ and $CO_2$ [29]. In this process, titania seems to have a barrier effect. Considering that $TiO_2$ is an inorganic compound with high thermal stability, it can be observed that the beads with Ti alone show higher thermal stability and lower mass losses compared to the composite beads with PAN.

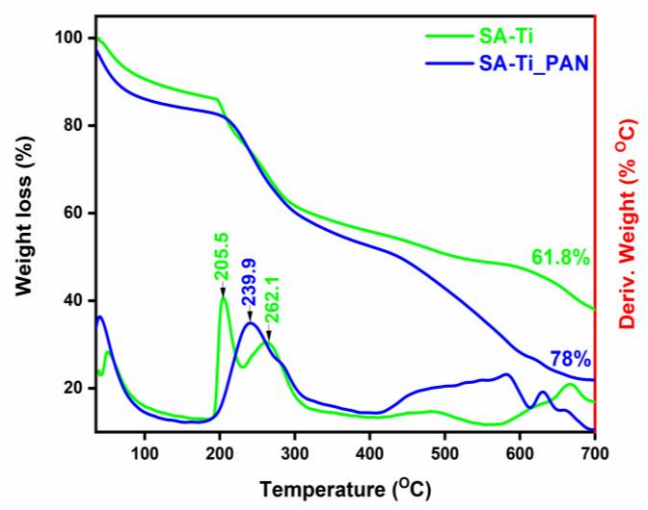


Fig 5. TGA/DTG curves for composite beads

### *3.2.3. Morphology of composites beads*

SEM images are relevant for determining the morphology of alginate and titania/composite beads. Both composite-based beads (Fig. 6(B)) and mesoporous titania-based beads (Fig. 6(D)) show a rather non-uniform surface. The surface roughness of the SA-Ti beads is higher and shows particle agglomerations compared to the SA-Ti_PAN sample. Yet, for SA-Ti_PAN beads a more homogeneous surface can be observed, with evenly dispersed particles. The appearance of veins on the surface is most likely due to polymer shrinkage in the $CaCl_2$ bath. Sectional SEM images confirm the presence of large aggregates of $TiO_2$ in the SA-Ti beads compared to the SA-Ti_PAN sample, which shows a more homogeneous inner texture with dispersed particles. The more homogenous

dispersion of $TiO_2$-PAN particles may be due to the presence of PAN of the surface of $TiO_2$, which acts as an interface that favours polymer-biopolymer interactions.

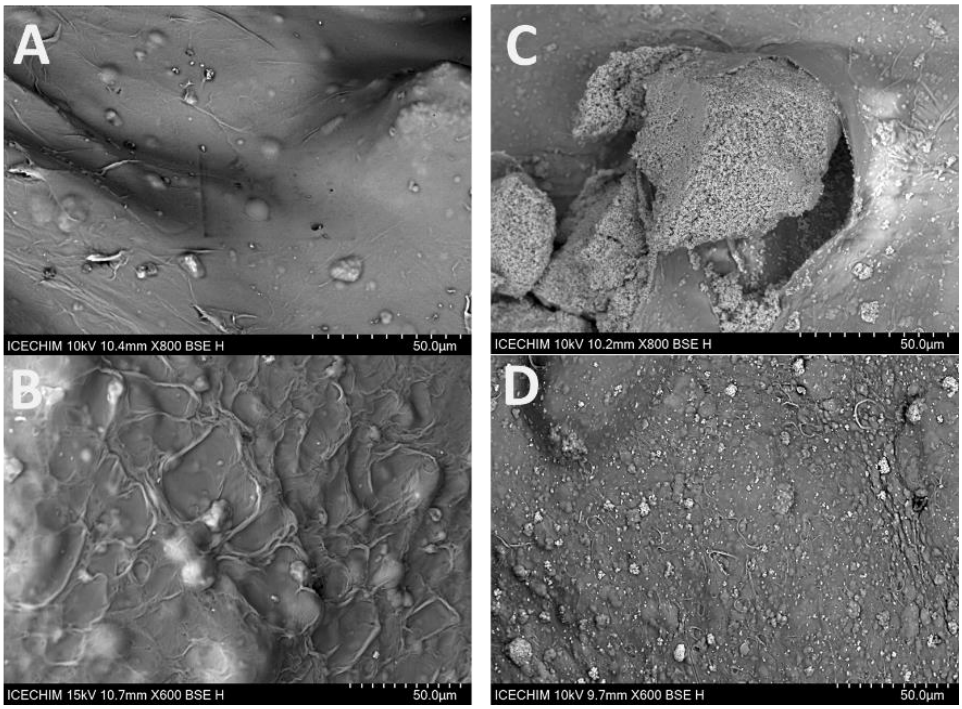


Fig 6. SEM images for SA-Ti_PAN (section A- 50 µm and surface B-50 µm) and SA-Ti (section C- 50 µm and surface D-50 µm)

### *3.2.4. Adsorption capacity of composite beads*

The need to determine the quantitative adsorption of heavy metals by the synthesized materials is necessary to rigorously determine the efficiency of the adsorption process. A variety of analytical techniques are available for the determination of heavy metal content, but they require prior sample preparation. Thus, the employed technique of quantitative determination by spectroscopy is more economic and less complex [30]. As a result, the amount of heavy metal adsorbed by the polymer beads was determined by XRF analysis. The percentage amount of heavy metal found in the polymer beads after adsorption is centralized in Table 4, while Fig. 7 highlights the specific signals of adsorbed heavy metals, as follows: Zinc shows a signal at a value of 8.6 keV, nickel 7.4 keV and copper at 8.04 keV.

Interestingly, it was observed that both samples show affinity for Cu ions, which was found in higher amounts relative to the other ions. It can also be noted that the overall capacity of SA-Ti_PAN to retain heavy metals is higher than the reference SA-Ti, by 24.89% for $Zn^{2+}$, 28.93% for $Ni^{2+}$ and 28.48% for $Cu^{2+}$.

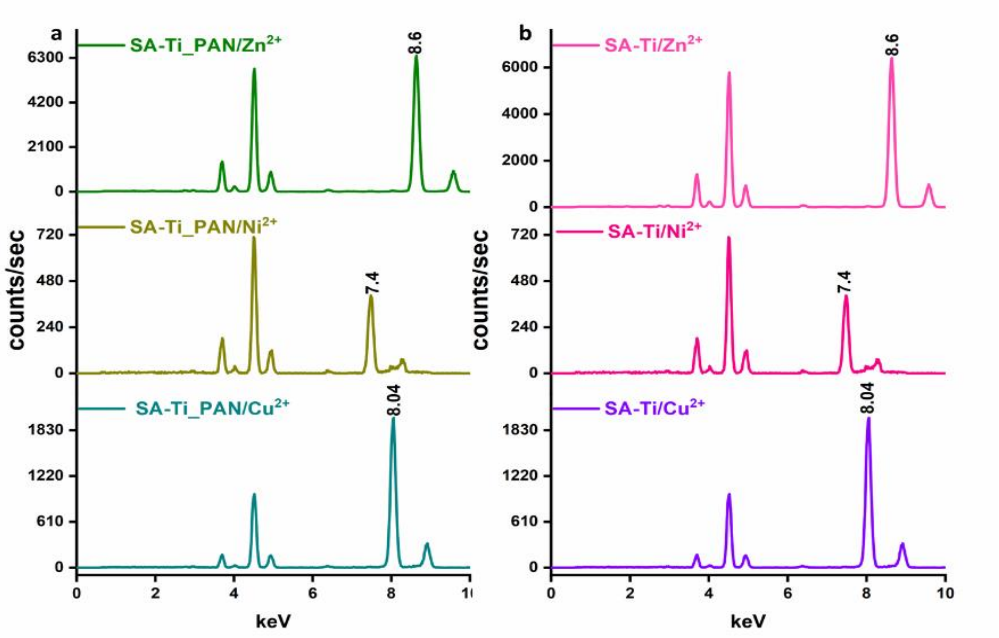


Fig 7. XRF spectra of SA-Ti_PAN (a) and SA-Ti (b) samples after adsorption of metal ions $Cu^{2+}$, $Ni^{2+}$, $Zn^{2+}$

*Table 4*

**Amount of heavy metal adsorbed by the polymer beads**

| Sample | Metal amount (%) |
|---|---|
| SA-Ti_PAN/$Zn^{2+}$ | 5.57 |
| SA-Ti_PAN/$Ni^{2+}$ | 6.05 |
| SA-Ti_PAN/$Cu^{2+}$ | 18.12 |
| SA-Ti/$Zn^{2+}$ | 4.46 |
| SA-Ti/$Ni^{2+}$ | 4.30 |
| SA-Ti/$Cu^{2+}$ | 12.96 |

## 4. Conclusions

In the first part of this study, an innovative host-guest method for obtaining inorganic-organic composites with improved properties was reported. In this respect, spectroscopy measurements confirmed the formation of the PAN polymer in the inorganic structure. According to the thermal analyses, performed on the obtained composites, the increase of the impregnation time leads to an increase of the mass loss, and, hence, of thermal stability. Although BET analysis showed a lower surface area and the Tg value was closer to the one of PAN, only $30MZ_{48}$-6hU was used for the following study on composite beads. This variant included less ultrasonication and polymerization times, which translates in reduced consumptions of energy and time.

The second stage of the study focused on developing hybrid composite beads based on mesoporous titania and inorganic-organic composite as fillers with applications for adsorption of heavy metals from water. Thus, hybrid beads based on alginate as organic matrix were compared to reference beads prepared using alginate and $TiO_2$ alone. The structure and composition of beads was underlined by FTIR spectroscopy and XRD analysis, which confirmed the presence of PAN in the composite beads but also revealed the crystalline anatase structure of $TiO_2$. Further on, TGA indicated that the mass loss of the SA-Ti sample is lower compared to that of the SA-Ti_PAN sample, which was additional proof that the $TiO_2$-PAN composite was quantitatively integrated in the alginate matrix, while SEM micrographs revealed a more homogenous surface and incorporation of $TiO_2$-PAN composites in the alginate matrix.

Finally, the heavy metal adsorption tests indicated that the alginate matrix has a higher affinity for Cu ions, relative to Zn and Ni ions, but also that SA-Ti_PAN retain all the three species of metal ions with over 25% efficiency relative to the reference beads with $TiO_2$ alone.

**Acknowledgments**

The results presented in this article have been funded by the Ministry of Investments and European Projects through the Human Capital Sectoral Operational Program 2014-2020, Contract no. 62461/03.06.2022, SMIS code 153735 and Project. no. 2N/03.01.2023 (PN 23.06.01.01.- AQUAMAT).

## R E F E R E N C E S

[1]. *Popuri, S. R., et al*., Removal of copper (II) ions from aqueous solutions onto chitosan/carbon nanotubes composite sorbent. DESALIN **52**, 691–701 (2014).

[2]. *Karkeh-abadi, F., et al*., The impact of functionalized CNT in the network of sodium alginate-based nanocomposite beads on the removal of Co(II) ions from aqueous solutions. J. Hazard. Mater. **312**, 224–233 (2016).

[3]. *Mousa, N. E., et al*., Regeneration of Calcium Alginate and Chitosan Coated Calcium Alginate Sorbents to be Reused for Lead (II) Removal from Aqueous Solutions. Rev. Chim. **68**, 1992–1996 (2017).

[4]. *Sarbu, A. et al*., Polymer inorganic- organic composites- precursors for ceramic powders and products. JESI **5**, 9–20 (2020).

[5]. *Sinha Ray, S. et al.*, Polymer/layered silicate nanocomposites: a review from preparation to processing. Prog. Poly. Sci. **28**, 1539–1641 (2003).

[6]. *Almeida, F. D., et al*., Compatibilization effect of organophilic clays in PA6/PP polymer blend. Procedia Manuf. **17**, 1154–1161 (2018).

[7]. *Porter, D., et al*., Nanocomposite fire retardants? a review. Fire Mater. **24**, 45–52 (2000).

[8]. *Radu, A.-L. et al*., New polymer inorganic-organic hybrids obtained through radical polymerization. U.P.B. Sci. Bull., Series B **73**, 1 (2011)

[9]. *Pomogailo, A. D.*, Hybrid Intercalative Nanocomposites. Inorg Mater **41**, S47–S74 (2005).

[10]. *Pu, Y. et al*., Low-temperature selective catalytic reduction of NOx with NH3 over zeolite catalysts: A review. Chin Chem Lett **31**, 2549–2555 (2020).

[11]. *Rao, C. N. R., et al*., Hybrid inorganic–organic materials: a new family in condensed matter physics. J. Phys.: Condens. Matter **20**, 083202 (2008).

[12]. *Duan, X., et al*., Functional Host–Guest Materials. in Modern Inorganic Synthetic Chemistry 493–543 (Elsevier, 2017)

[13]. *Wu, N., et al*., Efficient Removal of Heavy Metal Ions with Biopolymer Template Synthesized Mesoporous Titania Beads of Hundreds of Micrometers Size. Environ. Sci. Technol. **46**, 419–425 (2012).

[14]. *Shehzad, H. et al*., Modified alginate-chitosan-TiO2 composites for adsorptive removal of Ni(II) ions from aqueous medium. Int. J. Biol. Macromol. **194**, 117–127 (2022).

[15]. *Papageorgiou, S. K., et al*., Calcium alginate beads from Laminaria digitata for the removal of Cu+2 and Cd+2 from dilute aqueous metal solutions. Desalination **224**, 293–306 (2008).

[16]. *Wang, B. et al*., Alginate-based composites for environmental applications: A critical review. Crit. Rev. Environ. Sci. Technol.**49,** 318-356 (2018).

[17]. *Yang, N et al*., The Fabrication of Calcium Alginate Beads as a Green Sorbent for Selective Recovery of Cu(II) from Metal Mixtures. Crystals **255** (2019)

[18]. *Radu, A.-L. et al*., Unique polyvinyl acetate–mesoporous synthetic zeolite composites prepared in ultrasonic field. Microporous Mesoporous Mater. **198**, 281–290 (2014).

[19]. *Wang, J., et al*., Polyacrylonitrile/polyaniline core/shell nanofiber mat for removal of hexavalent chromium from aqueous solution: mechanism and applications. RSC Adv. **3**, 8978 (2013).

[20]. *Shaikh, S. F., et al*., D-sorbitol-induced phase control of TiO2 nanoparticles and its application for dye-sensitized solar cells. Sci Rep **6**, 20103 (2016).

[21]. *Ribeiro, R. F et al*., Thermal Stabilization study of polyacrylonitrile fiber obtained by extrusion. Polímeros **25**, 523–530 (2015).

[22]. *Yoshitomo F. et al*., Precursory reaction of thermal cyclization for polyacrylonitrile, Polymer, **226**, 123780, (2021)

[23]. *Daemi, H. et al*., Synthesis and characterization of calcium alginate nanoparticles, sodium homopolymannuronate salt and its calcium nanoparticles. Sci. Iran. **19**, 2023–2028 (2012).

[24].—*Rao, K. M*., Synthesis and Characterization of biodegradable Poly (Vinyl caprolactam) grafted on to sodium alginate and its microgels for controlled release studies of an anticancer drug. J. Appl. Pharm Sci.**3**, 061-069 (2013).

[25]. *Ali, N. et al*., Development and Characterization of Functionalized Titanium Dioxide-Reinforced Sulfonated Copolyimide (SPI/TiO2) Nanocomposite Membranes with Improved Mechanical, Thermal, and Electrochemical Properties. J Inorg Organomet Polym **30**, 4585–4596 (2020).

[26].—*Djerdj, I. et al*., Structural investigations of nanocrystalline TiO2 samples. J. Alloys Compd. **413**, 159–174 (2006).

[27]. *Bhagyaraj, S. et al*., Alginate-Mediated Synthesis of Hetero-Shaped Silver Nanoparticles and Their Hydrogen Peroxide Sensing Ability. Molecules **25**, 435 (2020).

[28].—*Kusuktham, B., et al*., Morphology and Property of Calcium Silicate Encapsulated with

Alginate Beads. Silicon **6**, 191–197 (2014).

[29].—*Salisu, A. et al*., Alginate graft polyacrylonitrile beads for the removal of lead from aqueous solutions. Polym. Bull. **73**, 519–537 (2016).

[30]. *Byers, et al.,* XRF techniques to quantify heavy metals in vegetables at low detection limits. Food Chem.: X **1**, 100001 (2019).